Article ID: 1000-324X(2019)11-1231-07 **DOI:** 10.15541/jim20190035

Deposition Temperature and Heat Treatment on Silicon Nitride Coating Deposited by LPCVD

LIAO Chun-Jing[1,2,3], DONG Shao-Ming[2], JIN Xi-Hai[2], HU Jian-Bao[2], ZHANG Xiang-Yu[2], WU Hui-Xia[1]

(1. College of Chemistry and Materials Science, Shanghai Normal University, Shanghai 200234, China; 2. Structural Ceramics and Composites Engineering Research Center, Shanghai Institute of Ceramics, Chinese Academy of Sciences, Shanghai 200050, China; 3. University of Chinese Academy of Sciences, Beijing 100049, China)

Abstract: Silicon nitride coatings on carbon fiber cloth were prepared by Low Pressure Chemical Vapor Deposition (LPCVD) from gas mixtures of $SiCl_4$-NH_3-H_2 at temperatures ranging from 750 ℃to 1250 ℃. The effects of deposition temperature on the growth kinetics, morphologies, chemical composition and bonding state of the coatings were investigated. The results showed that deposition rate increased monotonously with temperature up to 1050 ℃, then it reversely decreased. In the whole temperature range, the coating surface morphology became gradually coarse with cauliflower-like grains as the deposition temperature increased. The optimal deposition temperature for infiltration was in the range between 750 and 950 ℃. Chemical composition analysis demonstrated that the nitrogen content of the coating firstly decreased and then increased with temperature increase, while the silicon content continuously increased and the oxygen content gradually decreased in the whole temperature range. Heat treatment at 1300 ℃ and above crystallized the coating. Concurrently, a significant change in its surface morphology was observed. All heat-treated coatings were exclusively composed of α-Si_3N_4, without the presence of any β-Si_3N_4.

Key words: silicon nitride coating; growth kinetic; deposition temperature; chemical composition; heat treatment

Continuous fiber reinforced ceramic matrix composites (CMC) show great promise for use in high temperature thermal structural components, fusion and fission applications[1-2], because of their excellent characteristics such as high temperature oxidation resistance, low density, high specific strength, high specific modulus and excellent stability under irradiation[3-4]. As one crucial component of CMC, the interphase played an important role in determining the mechanical properties of materials by facilitating the operation of energy absorption mechanism such as fiber pull-out, interphase debonding and crack deflection[5-7]. Nowadays, the most widely used interphases were layer structured interphases, such as PyC and BN[8-10]. These interphases have weak interlayer bonding strength, which facilitates crack deflection and fiber pull-out during the fracture of the composite, thus absorbing the fracture energy and enhancing toughness of composites. While in many cases, multilayer interphase such as $(C/SiC)_n$ and $(BN/SiC)_n$ were also frequently used for oxidation resistance improvement of the composites[11-13]. However, the thermal expansion mismatch between SiC and C or BN was relatively large. The resulting thermal stress caused the formation of cracks in the multi-layer interphase, which partially offset its oxidation resistance. New type interphases of highly improved oxidation resistance are urgently needed for long-term service of CMC in high temperature oxidative atmosphere.

Si_3N_4 shows a lower oxidation rate than SiC in both dry and wet oxidative atmosphere[14-16]. The low thermal expansion mismatch between Si_3N_4 and C or BN is of particular importance[17], which can effectively alleviate the thermal stress within $(C/Si_3N_4)_n$ or $(BN/Si_3N_4)_n$ multilayer, thus preventing the formation of thermal cracks. At present, the effect of $(BN/Si_3N_4)_n$ interphase on the oxidation resistance of SiC/SiC composites was reported[18-20]. A significant improvement in the oxidation resistance was found.

The Si_3N_4 sublayer in the $(BN/Si_3N_4)_n$ multilayer interphase was generally prepared by Chemical Vapor In-

Received date: 2019-01-17; **Modified date:** 2019-03-11
Foundation item: National Key Research and Development Program of China (2016YFB0700202); National Natural Science Foundation of China (51872310); Chinese Academy of Science (QYEDY-SSW-JSC031)
Biography: LIAO Chun-Jing(1989–), male, candidate of Master degree. E-mail: lchj0123@163.com
Corresponding author: DONG Shao-Ming, professor. E-mail: smdong@mail.sic.ac.cn

filtration (CVI) method. For example, Liu, *et al*[21] deposited Si_3N_4 on fiber by using $SiCl_4$-NH_3-H_2-Ar system and the relevant thermodynamic analysis[22] have been conducted. However, few researches were conducted on the basic deposition process of Si_3N_4 sublayer on fiber. Especially, the influences of deposition temperature on the infiltration uniformity and elemental composition of coatings were rarely reported, which were critical steps for the multilayer interphase preparation and had great impact on not only the microstructure and property of the Si_3N_4 sublayer, but also those of the multilayer interphase as a whole. Moreover, the effect of crystallization degree of Si_3N_4 decreased the diffusion rate of gaseous products (N_2 and CO) under high temperature oxidizing environment[23], making it necessary to research the crystallization behavior at high temperature.

Based on the above consideration, LPCVD of Si_3N_4 on carbon fiber cloth was studied in the present work, using $SiCl_4$-NH_3-H_2 gas mixture as reactants. The influence of deposition temperature on the growth kinetics, morphology, chemical composition of the coatings on carbon fiber were investigated, together with its crystallization behavior and microstructure evolution during the heat treatment.

1 Experimental

1.1 Materials and preparation of the coatings

In the chemical vapor deposition system of $SiCl_4$-NH_3-H_2, the deposition was carried out in a horizontal hot-wall reactor with $SiCl_4$ delivered by H_2 from bubbler to the reactor *via* bubbling. In order to keep steady delivery of liquid $SiCl_4$ to reactor, the bubbler was heated by heating tape and maintained at 35 ℃. The deposition was proceeded at temperature from 750 ℃ to 1250 ℃, the total pressure in the reactor was maintained at 0.5 kPa. The flow rate of $SiCl_4$, NH_3 and H_2 were 40, 80 and 200 mL/min, respectively. In order to prevent the harmful pre-reaction between NH_3 and $SiCl_4$, these gases were separately transported through pipelines before their mixing in the hot zone.

1.2 Characterization

The surface and fracture morphologies of silicon nitride coatings were observed by scanning electron microscopy (SEM, SU8220, Hitachi, Japan). Phase composition of the coatings was characterized by X-ray diffraction (XRD, Ultima IV, Rigaku). The structures of the coatings were characterized by Fourier transform infrared spectroscopy (FT-IR, Nicolet Is10, Thermo Scientific). Chemical binding state and element content of the coatings were characterized by X-ray photoelectron spectroscopy (XPS, ESCAl ab250, Thermo Fisher Scientific).

2 Results and discussion

2.1 Growth kinetic

Fig. 1 shows the deposition rate of silicon nitride coating on the outer surface of the carbon fiber cloth. Obviously, the deposition rate showed a strong dependence on the temperature. The deposition rate firstly increased with temperature up to 1050 ℃, above which it reversely decreased up to 1250 ℃. The coating deposited at 1050 ℃ showed the largest thickness of about 30.2 μm, which was almost 43 times of that of the coating deposited at 750 ℃. The deposition activation energy was calculated using the Arrhenius equation[24]Eq.(1):

$$V_{dep} = A \cdot \exp(-E_a/RT) \quad (1)$$

Where V_{dep} refers to deposition rate, A pre-exponential factor, E_a apparent activation energy, R gas constant, T deposition temperature. According to the difference in activation energy, the whole plot could be divided into three regions, which corresponded to different deposition controlling mechanisms. During region I, a high activation energy of 159.6 kJ/mol was obtained according to Arrhenius equation, which demonstrated that the deposition was controlled by surface reaction, and surface processes such as surface adsorption, chemical reaction, surface atoms migration and desorption strongly depend on temperature. At high temperatures above 850 ℃ (Region II), a low activation energy of 129.7 kJ/mol was achieved. This was due to mass transfer through the boundary layer near the substrate surface[25]. Both regions complied well with the Arrhenius law, and showed an obvious deposition rate increased with temperature.

The deposition rate reached its maximum at 1050 ℃. When temperature further increased above 1050 ℃ (region III), an opposite trend of deposition rate variation was observed. The fact that deposition rate in this region declined dramatically with temperature was attributted to gas-phase nucleation, leading to the formation of a large amount of white powders during the deposition process.

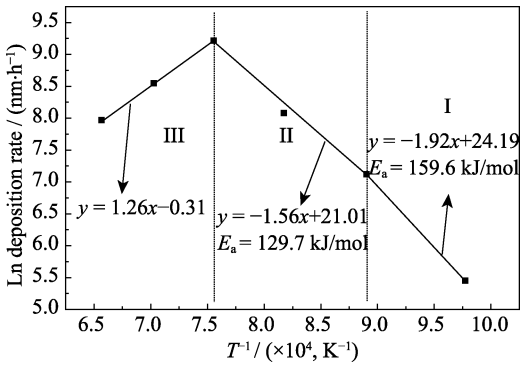

Fig. 1 Deposition rate as a function of temperature for $SiCl_4$-NH_3-H_2 system

The gas phase nucleation caused reactant molecules to nucleate and collide with each other and then absorb on the tube wall, which resulted in more reactants consumed in gas phase and made the reactants less available on the substrate surface for coating deposition.

2.2 Surface and fracture morphologies of coatings

Fig. 2 shows the morphologies of the original and silicon nitride coated carbon fiber surfaces. The original carbon fiber surface was densely populated with deep grooves that parallelly aligned along the fiber axis. Such a scene was also found in T300 carbon fiber surface[25], and was the inherent characteristic of carbon fiber surface. After the fiber coated with silicon nitride was deposited at 750 ℃, its surface became very smooth without any obvious defects. At this time, the surface grooves had been completely filled with silicon nitride, although the inter-fiber gaps between nearby fibers were still clearly distinguishable. Similar phenomenon was observed for the fiber deposited at 850 ℃, except that a large number of small cauliflower-like particles appeared on the fiber surface. However, when the deposition temperature of silicon nitride coating increased to 950 ℃ and above, great changes in the fiber surface morphology occurred. Large cauliflower-like particles presented on the fiber surface, which continuously grew in size with temperature, suggesting the particles undergo the process of growth. Correspondingly, the fiber surface became increasingly coarse, along with nearly complete filling of inter-fiber gaps by silicon nitride. This phenomenon agreed well with the very fast deposition rate and hereby the large thickness of the silicon nitride coating as shown in Fig. 1.

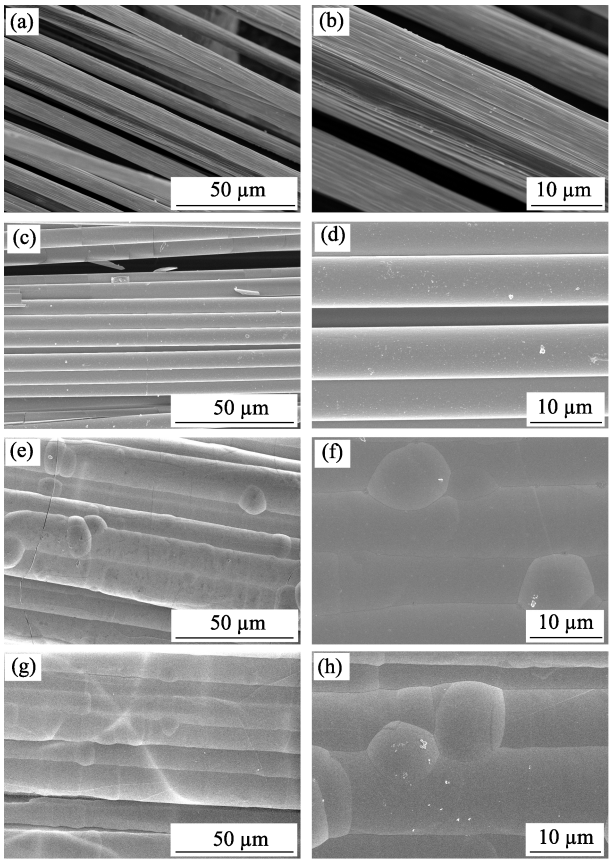

Fig. 2　Surface morphologies of silicon nitride coatings coated carbon fiber cloth at different temperatures
(a, b) Original; (c, d) 750 ℃; (e, f) 950 ℃; (g, h) 1150 ℃

Fig. 3 shows the fracture morphologies of silicon nitride coating coated the carbon fiber cloth at different temperatures. As shown in Fig. 3, the thickness difference between outer coatings and inner coating showed strong dependence on the deposition temperature. The sample deposited at 750 ℃ showed thin outer and inner coating of 700 and 300 nm, respectively. The thickness difference small. When the deposition temperature increased to 850 ℃, a significant increase in the outer and inner coating thickness occurred. In this case, the sample showed relatively large outer and inner coating thickness of 3.7 μm and 800 nm, while the coating thickness difference still kept moderate. However, further increase in the deposition temperature to 950 ℃ and above resulted in a radical increase in the thickness difference. At this time, the coating was mainly deposited on the outer surface of fiber preform with little deposit infiltrating into its interior, leading to a continuous increase in the outer coating thickness but a gradual decrease in the inner coating thickness. Taken the sample deposited at 950 ℃ for example, this sample showed an outer coating thickness of 9.67 μm, much more thick than that of the sample deposited at 850 ℃; while its inner coating thickness was only 500 nm, greatly thinner in comparison with that of the sample deposited at 850 ℃. The strong deposition temperature dependence of the inner and outer coating thickness could be understood by using the dimensionless infiltration Peclet number (Pe_i)[26], which was used to compare the mass transfer by diffusion inside the fibrous preform and convection outside the fibrous preform. As Pe_i increased with increasing temperature, the convection mass transfer outside the preform would gradually become dominant in comparison with the diffusion mass transfer inside the preform as the deposition temperature increased. Therefore, the reaction product was prevalently deposited on the exterior surface of preform, leading to a rapid growth of outer coating rather than the inner coating. Moreover, with the rapid growth of outer coating at high temperature, premature blockage of pores on the preform surface could even occur, which further exaggerated the growth rate difference between the inner and outer coatings. As a result, a strong deposition temperature dependence of the inner and outer coatings' thickness was observed.

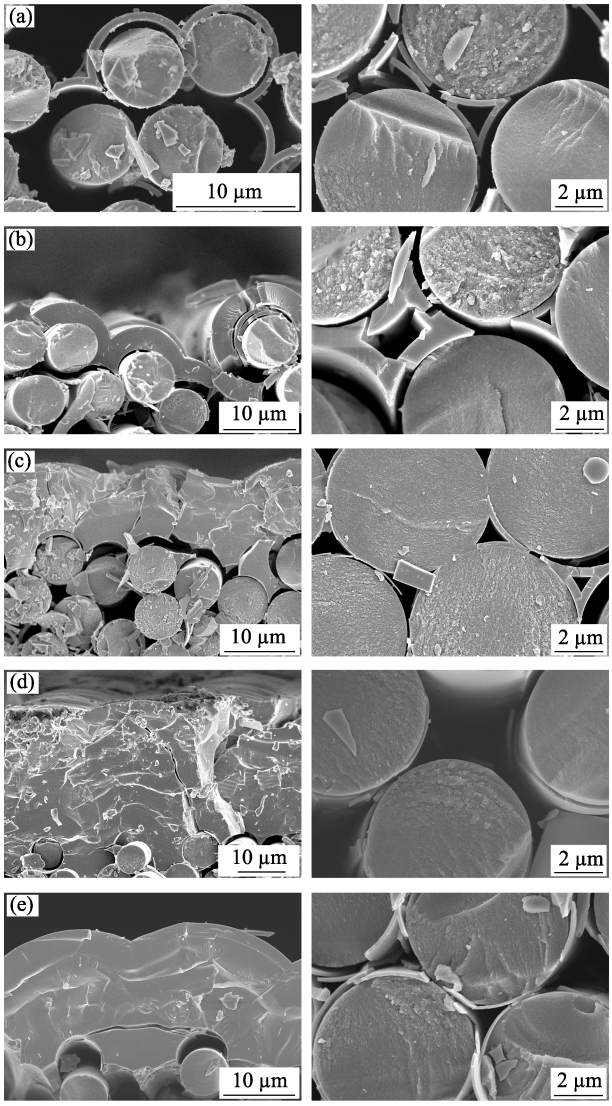

Fig. 3 Fracture morphologies of silicon nitride deposited on the carbon fiber cloth at different temperatures

The left figures show outer coating morphologies of carbon fiber cloth while the right figures show their corresponding inner coating morphologies: (a) 750 ℃; (b) 850 ℃; (c) 950 ℃; (d) 1050 ℃; (e) 1150 ℃

2.3 Chemical composition

XPS analysis of coatings was conducted on silicon nitride coatings deposited from 750 ℃ to 1150 ℃, and the results were given in Table 1.

Table 1 Chemical composition of silicon nitride deposited at different temperatures

Deposition temperature/℃	Elemental type and elemental contents/at%		
	N	Si	O
750	53.21	30.78	16.01
850	46.92	43.25	9.82
950	43.67	43.49	12.84
1050	50.43	43.60	5.97
1150	49.88	46.87	3.24

These coatings mainly consisted of three elements, N, Si and O. The nitrogen content decreased monotonously from 53.21at% to 43.67at% as the deposition temperature increased from 750 ℃ to 950 ℃. Above 950 ℃, a reverse increase of the nitrogen content occurred. The nitrogen content of the samples deposited at 1050 ℃ increased to about 50at% and remained nearly constant with the increasing temperature. As for the silicon and oxygen contents, they were quite different. The silicon content showed a monotonic increase from 30.78at% to 46.87at% with the deposition temperature raised from 750 ℃ to 1150 ℃, while an opposite tendency was observed for the oxygen content. The oxygen content showed a nearly continuous decrease with the deposition temperature from 16.01at% to 3.24at%. It was quite notable that the oxygen content in the coatings was considerably high, especially for the samples prepared at low temperatures. In fact, such a phenomenon was frequently observed in the CVD silicon nitride films as reported by many previous researchers[27-28].

Fig. 4 shows the N1s and Si2P XPS spectra of silicon nitride coating deposited at different temperatures. For all coatings, the bonding states of nitrogen were almost the same independent of the deposition temperature. The XPS spectrum of nitrogen can be fitted with two sub-peaks located at 397.4 and 399.28 eV, which corresponded to N–Si and N–O bonds, respectively[29-30]. No sub-peak was found at 400.6 eV, suggesting that there was no N–H bond in the coating[31]. For the sample deposited at 750 ℃, the N1s spectrum was highly asymmetrical. The strong N–O sub-peak caused the appearance of a shoulder on this spectrum, because of the high oxygen content in the coating. While for other samples, the N1s spectra were more symmetrical. In these cases, the whole N1s spectrum was composed of a strong N–Si main peak in company with a weak N–O sub-peak. The intensity of the N–O sub-peak decreased with the increase of deposition temperature, which was in consistence with the continuous reduction of oxygen content in the sample.

As to the Si2p spectrum, the sample deposited at 750 ℃ only exhibited a single main peak at 101.5 eV, which was ascribed to N–Si bond of silicon nitride[28]. However, when the deposition temperature was raised to 950 and 1150 ℃, an extremely weak sub-peak appeared at 99.5 eV apart from the N–Si main peak. This sub-peak corresponded to silicon in the sample[29], its content was less than 5at%. Furthermore, it was quite a surprise that for all samples, no sub-peak at 103.5 eV corresponding to Si–O bond[28] was observed in their Si2p spectra despite the unequivocal existence of oxygen in these samples. The reasons for that are still unclear, and further investigation is necessary.

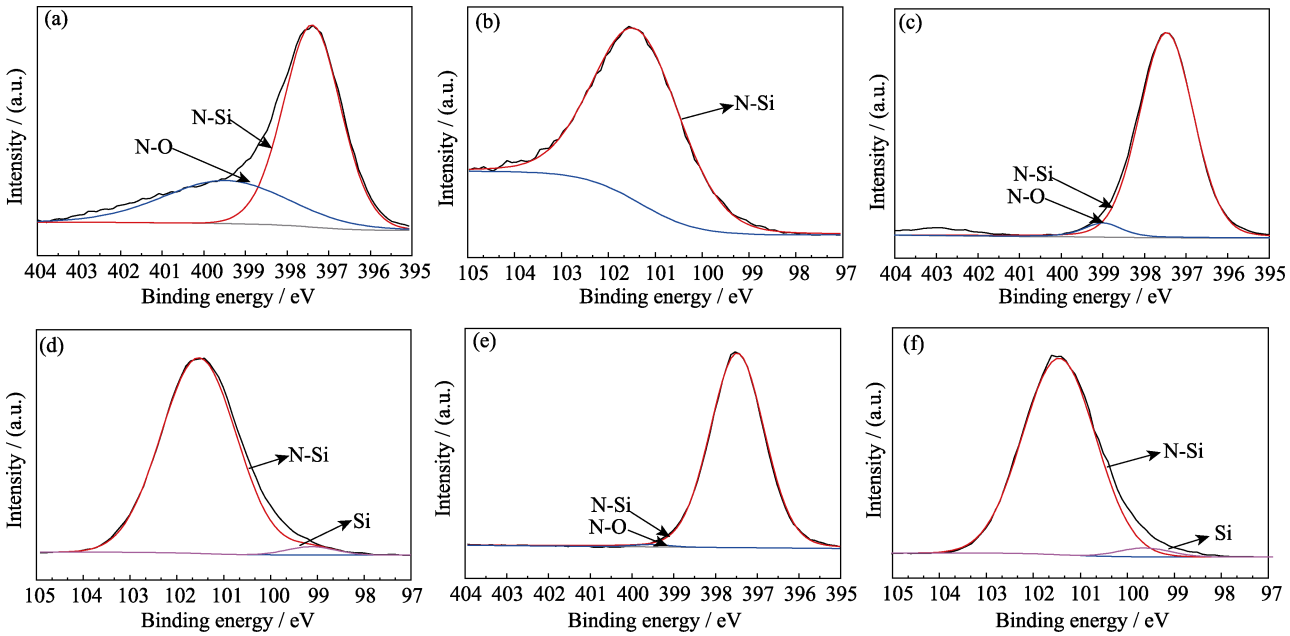

Fig. 4　N1s and Si2P XPS spectra of silicon nitride coatings deposited at different temperatures
(a-b) 750 ℃; (c-d) 950 ℃; (e-f) 1150 ℃; (a, c, e) NIS spectra; (b, d,f) Si2P spectra

2.4　Effect of heat treatment on the structure of coatings

Silicon nitride coatings deposited from $SiCl_4$-NH_3-H_2 below 1300 ℃ was usually amorphous structure. In order to increase the crystallinity, the chemical vapor deposited coatings were heat-treated in Ar for 2.5 h under gas pressure of 0.1 MPa, Fig. 5 shows the FT-IR spectra of as-deposited and heat-treated coatings. All the coatings showed an absorption band at around 900 cm^{-1} along with a minor absorption band at around 500 cm^{-1}, which were attributed to the asymmetrical stretching vibration and symmetrical stretching vibration of Si–N–Si bonds, respectively[32]. No absorption bands ascribing to N–H, Si–Cl or Si–H bond vibrations were observed, indicating the complete decomposition of reactants. The as-deposited coating showed broad absorption bands, which implied the as-deposited coating had low crystallinity. After heat treatment, the adsorption bands became increasingly sharp and narrow, as a result of the increased coating crystallinity. For the sample heat treated at 1400 and 1500 ℃, even distinctive band splitting occurred. The broad absorption bands centered at around 900 and 500 cm^{-1} split into well separated tiny bands of high sharpness, and concurrently the whole bands shifted to high frequencies. The tiny bands located at 600, 495, 460 and 406 cm^{-1} were in good agreement with the characteristic adsorption bands of α-Si_3N_4, no tiny sharp bands of β-Si_3N_4 at 578 and 443 cm^{-1}[33] were found, indicating that the coatings after heat treatment were composed of α-Si_3N_4.

In order to further testify the crystallization behavior of the coating, XRD patterns were conducted on coatings heat treated at different temperatures, as given in Fig. 6. The coating heat-treated at 1300 ℃ showed six diffraction peaks at around 2θ=20.54°, 22.90°, 30.88°, 34.48°, 35.20°, 38.78°, which were due to the reflections of (101), (110), (201), (102), (210) and (211), respectively. However, the diffractions were still weak as compared with α-Si_3N_4 without other diffraction peaks, suggesting that the coating were partially crystallized. When heat-treatment temperature was increased to 1400 ℃, the intensities of these diffraction peaks increased and full width at half maximum (FWHM) decreased together with the appearance of new peaks, which was a direct indication of the further improvement in the crystallinity of the coatings. Besides above-mentioned diffraction peaks, heat treatment temperature increasing to 1500 ℃ resulted in appearance of other diffraction peaks at around 2θ=46.86°(220), 59.51°(312), 59.94°(320), 68.08°(104), 74.75°(420). Moreover, all the diffraction peaks were in consistence with those of α-Si_3N_4 (PDF#09-0250), which further confirmed the exclusive crystallization of the coating into α-Si_3N_4, as revealed by FT-IR.

Fig. 7 shows the surface morphology of the coating heat treated at 1500 ℃. Great changes in the coating morphology could be observed in comparison with the as-deposited coatings prepared at 850 ℃. The coating surface became obviously rough and grainy, with extruding silicon nitride grains 1–2 μm in diameter clearly visible. The changes in morphology meant the migration and recrystallization of atoms, which was consistent with the results from FT-IR and XRD analysis that the amorphous silicon nitride became well crystallized after 1500 ℃ heat treatment. In addition, due to the volume shrinking

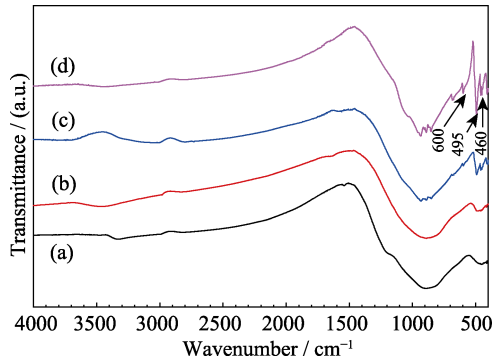

Fig. 5 FT-IR spectra of silicon nitride coatings heat-treated at different temperatures
(a) As-deposited; (b) 1300 ℃; (b) 1400 ℃; (d) 1500 ℃

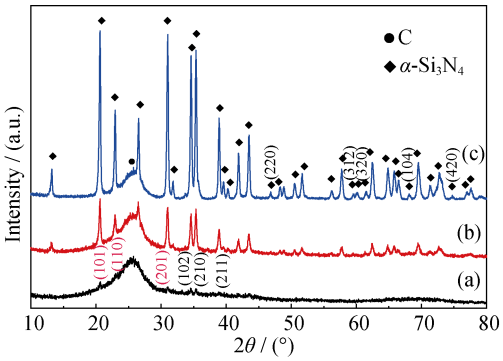

Fig. 6 XRD patterns of as-deposited coatings heat-treated at different temperatures
(a) 1300 ℃; (b) 1400 ℃; (c) 1500 ℃

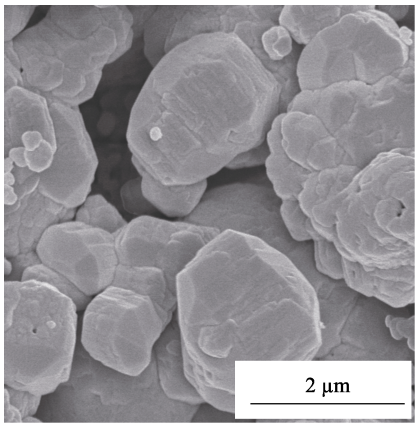

Fig. 7 Surface morphology of silicon nitride coating deposited at 850 ℃ followed by heat treatment at 1500 ℃ for 2.5 h in Ar

accompanied with silicon nitride crystallization, pores formed in the coating, making it look more porous. Such changes in the microstructure and crystallinity of the coating might have a strong influence on its mechanical and oxidation resistance properties, as will be studied later.

3 Conclusions

Chemical vapor deposition of silicon nitride was investigated, using carbon fiber cloth as substrate, and $SiCl_4$-NH_3-H_2 as gas phase reactants. It was found that temperature had a strong influence on the deposition rate and controlling mechanism of silicon nitride deposition. The deposition process was mainly controlled by surface reaction below 850 ℃, while it was controlled by mass transport at 850–1050 ℃. The deposition rate increased with temperature, and reached maximum at 1050 ℃. Above this temperature, a reverse decrease in the deposition rate occurred. Meanwhile, remarkable changes in the chemical composition and surface morphology of the coating were observed. The coating surface became gradually rough as the deposition temperature increased. At the same time, the nitrogen, silicon and oxygen content showed different vibration trend. The as-deposited coating was amorphous in nature, and crystallized into α-Si_3N_4 after heat treatment at 1300–1500 ℃.

References:

[1] OHNABE H, MASAKI S, ONOZUKA M, *et al*. Potential application of ceramic matrix composites to aero-engine components. *Composites Part A-Applied Science and Manufacturing*, 1999, **30(4):** 489–496.
[2] KATOH Y, SNEAD L L, HENAGER C H, *et al*. Current status and critical issues for development of SiC composites for fusion applications. *Journal of Nuclear Materials*, 2007, **367–370(part A):** 659–671.
[3] CHRISTIN F. Design, fabrication, and application of thermostructural composites (TSC) like C/C, C/SiC, and SiC/SiC composites. *Advanced Engineering Materials*, 2012, **4(12):** 903–912.
[4] DONALD I W, MCMILLAN P W. Ceramic-matrix composites. *Journal of Materials Science*, 1976, **11(5):** 949–972.
[5] THOULESS M D, EVANS A G. Effect of pull-out on the mechanical properties of ceramic-matrix composites. *Acta Metallurgica*, 1988, **36(3):** 517–522.
[6] NASLAIN R R, PAILLER R J F, LAMON J L. Single- and multilayered interphase in SiC/SiC composites exposed to severe environmental conditions: an overview. *International Journal of Applied Ceramic Technology*, 2010, **7(3):** 263–275.
[7] BERTRAND S, PAILLER R, LAMON J. Influence of strong fiber/coating interfaces on the mechanical behavior and lifetime of Hi-NICALON/(PyC/SiC)$_n$/SiC minicomposites. *Journal of The American Ceramic Society*, 2001, **84(4):** 787–794.
[8] WANG DENG-KE, DONG SHAO-MING, ZHOU HAI-JUN, *et al*. Effect of pyrolytic carbon interface on the properties of 3D C/ZrC–SiC composites fabricated by reactive melt infiltration. *Ceramics International*, 2016, **42(8):** 10272–10278.
[9] CHENG YU, YIN XIAO-WEI, LIU YONG-SHENG, *et al*. BN coatings prepared by low pressure chemical vapor deposition using boron trichloride-ammonia-hydrogen-argon mixture gases. *Surface and Coatings Technology*, 2010, **204(16/17):** 2797–2802.
[10] MA XIAO-KANG, YIN XIAO-WEI, CAO XIAO-YUN, *et al*. Effect of heat treatment on the mechanical properties of SiC$_f$/BN/SiC fabricated by CVI. *Ceramics International*, 2016, **42(2):** 3652–3658.
[11] YU HAI-JIAO, ZHOU XING-GUI, ZHANG WEI, *et al*. Mechanical behavior of SiC$_f$/SiC composites with alternating PyC/SiC multilayer interphases. *Materials and Design*, 2013, **44(1):** 320–324.
[12] PASQUIER S, LAMON J, NASLAIN R. Tensile static fatigue of 2D SiC/SiC composites with multilayered (PyC–SiC)$_n$ interphases at high temperatures in oxidizing atmosphere. *Composites*

Part A-Applied Science and Manufacturing, 1998, **29(9/10):** 1157–1164.
[13] NIIHARA K, NAKANO K, SEKINO T, *et al*. $(PyC/SiC)_n$ and $(B/N/SiC)_n$ nanoscale-multilayered interphases by pressure pulsed-CVI. *Key Engineering Materials*, 1998, **164–165:** 357–360.
[14] OGBUJI L U J T, OPILA E J. A comparison of the oxidation kinetics of SiC and Si_3N_4. *Journal of The Electrochemical Society*, 1995, **142(3):** 925–930.
[15] OPILA E J, HANNJR R E. Paralinear oxidation of CVD SiC in water vapor. *Journal of The American Ceramic Society*, 1997, **80(1):** 197–205.
[16] FOX D S, OPILA E J, NGUYEN Q N, *et al*. Paralinear oxidation of silicon nitride in a water-vapor/oxygen environment. *Journal of The American Ceramic Society*, 2003, **86(8):** 1256–1261.
[17] MOORE A W, SAYIR H, FARMER S C, *et al*. Improved Interface Coatings for SiC Fibers in Ceramic Composites, in: J.B. Wachtman, Proceedings of the 19th Annual Conference on Composites, Advanced Ceramics, Materials, and Structures-A. The American Ceramic Society, Westerville, 1995, **16:** 409–416.
[18] KMETZ M. Multilayered Boron Nitride/Silicon Nitride Fiber Coatings. United States, Patent 7510742. 2009.03.31.
[19] HILL C L. Interface and Matrix Processing Evaluation for Non-oxide Ceramic Matrix Composites. Storrs: PhD Thesis of University of Connecticut, 2009.
[20] COONS T P, REUTENAUER J W, FLANDERMEYER B, *et al*. An investigation into a multilayered $BN/Si_3N_4/BN$ interfacial coating. *Journal of Materials Science*, 2013. **48(18):** 6194–6202.
[21] LIU YONG-SHENG, CHENG LAI-FEI, ZHANG LI-TONG, *et al.* Preparation and characterization of C/Si_3N_4 composites by chemical vapor infiltration. *Journal of Inorganic Materials*, 2005, **20(5):** 1208–1214.
[22] REN HAI-TAO, ZHANG LI-TONG, SU KE-HE, *et al*. Thermodynamic study on the chemical vapor deposition of silicon nitride from the $SiCl_4$–NH_3–H_2 system. *Computational and Theoretical Chemistry*, 2015, **1051:** 93–103.
[23] LUTHRA K L. Theoretical Aspects of the Oxidation of Silica-forming Ceramics, in: K.G. Nickel. Corrosion of Advanced Ceramics. Netherlands: Springer, 1993**:** 23–34.
[24] LIU YONG-SHENG, ZHANG LI-TONG, CHENG LAI-FEI, *et al*. Effect of deposition temperature on boron-doped carbon coatings deposited from a BCl_3-C_3H_6-H_2 mixture using low pressure chemical vapor deposition. *Applied Surface Science*, 2009, **255(21):** 8761–8768.
[25] LI JUN-SHENG, ZHANG CHANG-RUI, LI BIN. Preparation and characterization of boron nitride coatings on carbon fibers from borazine by chemical vapor deposition. *Applied Surface Science*, 2011, **257(17):** 7752–7757.
[26] CHOLET V, VANDENBULCKE L. Chemical vapor infiltration of boron nitride interphase in ceramic fiber preforms: discussion of some aspects of the fundamentals of the isothermal chemical vapor infiltration process. *Journal of The American Ceramic Society*, 1993, **76(11):** 2846–2858.
[27] YANG G R, ZHAO Y R, HU Y Z, *et al*. XPS and AFM study of chemical mechanical polishing of silicon nitride. *Thin Solid Films*, 1998, **333(1/2):** 219–223.
[28] LIU XUE-JIAN, CHEN YAO-FENG, LI HUI-LI, *et al*. Preparation and characterization of low pressure chemically vapor deposited silicon nitride thin films from tris (diethylamino) chlorosilane and ammonia. *Thin Solid Films*, 2005, **479(1/2):** 137–143.
[29] POON M C, KOK C W, WONG H, *et al*. Bonding structures of siliconoxynitride prepared by oxidation of silicon-rich silicon nitride. *Thin Solid Films*, 2004, **462–463:** 42–45.
[30] LI JIAN-PING, QIN HAI-LONG, LIU YONG-SHENG, *et al*. Effect of the $SiCl_4$ flow rate on SiBN deposition kinetics in $SiCl_4$-BCl_3-NH_3-H_2-Ar environment. *Materials*, 2017, **10(6):** 627–637.
[31] LAIDANI N, ANDERLE M, CANTERI R, *et al*. Structural and compositional study of B-C-N films produced by laser ablation of B_4C in N_2atmosphere. *Applied Surface Science*, 2000, **157(3):** 135–144.
[32] NIIHARA K, HIRAL T. Chemical vapour-deposited silicon nitride: Part 3 Structural Features. *Journal of Materials Science*, 1977, **12(6):** 1233–1242.
[33] LUONGO J P. Infrared Characterization of α- and β- crystalline silicon nitride. *Journal of the Electrochemical Society*, 1983, **130(7):** 1560–1561.

沉积温度及热处理对低压化学气相沉积氮化硅涂层的影响

廖春景[1,2,3]，董绍明[2]，靳喜海[2]，胡建宝[2]，张翔宇[2]，吴惠霞[1]

(1. 上海师范大学 化学与材料科学学院，上海 200234; 2. 中国科学院 上海硅酸盐研究所，结构陶瓷与复合材料工程研究中心，上海 200050; 3. 中国科学院大学，北京 100049)

摘 要: 以 $SiCl_4$-NH_3-H_2 为前驱体，在 750~1250 ℃范围内通过低压化学气相沉积技术于碳纤维布上制备氮化硅涂层，系统研究了沉积温度对氮化硅涂层的生长动力学、形貌、化学组成和结合态的影响。研究结果表明，在沉积温度低于1050 ℃的情况下，随着沉积温度的升高，沉积速率单调增大。而当沉积温度高于1050 ℃时，沉积速率随温度升高逐渐下降。在整个沉积温度范围内，随着沉积温度的升高，涂层表面形态逐渐向菜花状转变，同时涂层表面变得愈加粗糙。涂层的最佳沉积温度在 750~950 ℃之间。随着沉积温度的升高，涂层中氮含量先降低后升高，而硅含量不断增加，氧含量在整个温度范围内逐渐降低。原始沉积涂层均呈无定形态，经高于 1300 ℃热处理后实现晶化，并伴随着表面形貌的显著变化。此时涂层仅由 α-Si_3N_4 构成，不存在任何 β-Si_3N_4 相。

关 键 词: 氮化硅涂层；生长动力学；沉积温度；化学组成；热处理

中图分类号: TQ174　　**文献标识码:** A